Turbulent Bursts in Couette-Taylor Flow

K. Coughlin
Université de Montréal, Montréal, Canada H3C 3J7

P. S. Marcus
University of California, Berkeley, California 94720
(Received 31 October 1994; revised manuscript received 7 March 1996)

We present a physical explanation of turbulent bursts in the flow between concentric, rotating cylinders (Couette-Taylor flow), based on fully resolved direct numerical calculations. The bursts are a temporal oscillation between a spatially laminar flow and turbulence, discovered experimentally by Hamill *et al.* The onset of turbulence is shown to be due to a linear instability of the spiral flow, discovered in our calculations and since confirmed experimentally. [S0031-9007(96)00971-4]

PACS numbers: 47.20.Ky, 47.20.Lz, 47.27.Cn, 47.27.Nz

We present a study of a flow with space-filling turbulent bursts, i.e., one that oscillates in time between laminar and turbulent states. Here, we use the terms laminar and turbulent to denote spatially coherent, slowly evolving, ordered flow patterns vs spatially disordered, rapidly fluctuating states. Bursts are interesting because they provide an example, of phenomena typical of the onset of turbulence in shear flows—subcritical transition and spatial and temporal intermittency. These phenomena are difficult to model realistically using the usual tools of perturbation theory, and so a general theory of transition to turbulence has yet to be constructed. In this paper, by examining a simple but experimentally realizable flow, we show that turbulent bursts occur in cycles of a well-defined sequence of steps. We offer physical and/or mathematical explanations for each step. In particular, we show that the onset of turbulence is directly linked to a secondary instability of the laminar flow, and explain the repeated collapse of the turbulence. Our resulting conceptual model is general enough to apply to turbulent bursts in a much wider context.

The first experiments showing turbulent bursts (limited in both space and time) in Couette-Taylor (CT) flow were by Coles [1] and Andereck *et al.* [1]. Space-filling turbulent bursts, the focus of this paper, were discovered experimentally by Hamill *et al.* [2]. In CT flow the fluid is confined between two concentric, independently rotating cylinders. The flow geometry is defined by the cylinders' radius ratio $\eta = a/b$ and aspect ratio $\Gamma = H'/(b - a)$, where H', a, and b are the height and inner and outer radii of the cylinders. Typically, CT flows are nearly periodic in the axial direction, and nearly independent [1,2] of Γ for $\Gamma \gtrsim 20$; hence, calculations that impose axial periodicity usually have good agreement with laboratory experiments [3,4]. The control parameters are $\mu \equiv \Omega_a/\Omega_b$ where Ω_a and Ω_b are the inner and outer cylinder rotation rates, and a Reynolds number $R \equiv (b - a)|b\Omega_b - a\Omega_a|/\nu$, where ν is the kinematic viscosity. Experimentally [2], turbulent bursts were found for counterrotating cylinders with $\mu = -2.797$ and $\eta = 0.799$ and over a range of R. In this range, the laminar part of the flow's cycle looks and behaves like "interpenetrating spiral" (IPS) [1] flow (described below). The IPS flow is spatially organized, but power spectra of scattered light intensity show broad peaks, indicating that the flow is temporally chaotic [1,2]. The IPS flow is interrupted by space-filling bursts of turbulence, and the onset and collapse of this turbulence is cyclic in time. The mean duration T and standard deviation σ of the cycle decrease with increasing R, and for sufficiently large R the flow remains turbulent for all time.

Numerically, we have calculated turbulent bursts by solving the Navier-Stokes equations using a spectral initial-value code which has excellent agreement with laboratory flows [3,4]. The main difference between the numerical calculations and laboratory experiments is that the former imposes wavelength H in the axial (z) direction. As expected, this leads to some differences between the laboratory and computed flow states [5]; however, these are quantitative rather than qualitative. Thus, we can gain an understanding of turbulent bursts by examining the bifurcations that occur as R is increased *when axial periodicity is imposed.* For R less than a critical value R_c, the primary circular Couette flow is a function only of radius (r) and is stable with $\mathbf{v} = V(r)\hat{\mathbf{e}}_\phi$, where $V(r)$ is determined by the boundary conditions [6]. Circular Couette flow is centrifugally unstable to the formation of Taylor vortices wherever $dL^2/dr < 0$, where $L(r) = rV(r)$ is the angular momentum per unit mass of the fluid [6]. When $\mu < 0$, a nodal surface exists at $r = r^*$ such that $V(r^*) = 0$; this surface divides the flow into two regions. For $r < r^*$ (the "inner region") the gradient $dL^2/dr < 0$, and the flow is centrifugally unstable, while for $r > r^*$ (the "outer region"), $dL^2/dr > 0$, and the flow is stable. For $\mu = -2.797$ and $\eta = 0.799$, our calculations show that there is a supercritical Hopf bifurcation at $R_c = 2116.6$ [7]. The eigenmodes associated with this bifurcation have the form $\mathbf{f}(r)e^{st}e^{i[2\pi z/\lambda + m(\phi - ct)]}$, where the growth rate s and phase speed c are real. If $m = 0$, then $c = 0$, but for

 0031-9007/96/77(11)/2214(4)$10.00

$\mu < 0$ the most unstable eigenmodes have $m \neq 0$ and $c \neq 0$. Modes with $m > 0$ ($m < 0$) have the symmetry of left- (right-) handed spirals. These left- and right-handed spiral eigenmodes are degenerate, having the same $\mathbf{f}(r)$, s, c, and critical values R_c, λ_c, and $|m_c|$. For $\mu = -2.797$ and $\eta = 0.799$, $m_c = 4$ and $\lambda_c = 1.0856$. [We use dimensionless units where the fluid density, gap width $(b - a)$, and inner cylinder speed $|\Omega_a|a$ are equal to unity.] The phase speed c is positive and approximately independent of m, λ, μ, and R. For the most unstable eigenmodes, $c \simeq 0.3\Omega_a$ which is approximately the value of $V(r)$ at the r where the eigenmode has its maximum amplitude. This radius is less than r^* (the eigenmode is exponentially small for $r > r^*$), so the spiral rotates in the same direction as the inner cylinder.

Our calculations with R slightly greater than R_c show that an initial condition consisting of a single eigenmode evolves to nonlinear spiral Taylor vortex flow with the form

$$\mathbf{v}_{\mathrm{sv}} = \sum_{n=-\infty}^{\infty} \mathbf{a}_n(r) e^{in[2\pi z/\lambda + m(\phi - ct)]} \qquad (1)$$

The helicity of the final flow (determined by the sign of m) depends on the initial conditions, and once established a spiral of one helicity is stable to perturbations of opposite helicity. Spiral vortex flow consists of a pair of counter-rotating vortices confined to $r < r^*$ [Fig. 1(a)]. In the outer region the flow remains approximately azimuthal, is not centrifugally unstable, and physically resembles a parallel shear flow. We define a Reynolds number for this outer region, $R_{\mathrm{outer}} = |\Omega_b|b(b - r^*)/\nu$, which has values between 1200 and 1500. This is in the same range where channel flow is observed to be subcritically unstable to the onset of turbulence [8].

Numerically as R is increased, spiral vortex flow becomes unstable to the temporally chaotic, but spatially ordered, IPS flow. The chaos is due to mode competition among the unstable eigenmodes of circular Couette flow that have different values of m and λ. For example, at $R = 1.18R_c$, eigenmodes with $|m| = 2$, 4, and 6 (for $\lambda = 0.90$) are unstable. A fully nonlinear calculation initialized with an arbitrary combination of these eigenmodes does not settle into a spiral vortex flow with a unique spiral structure, although long sections of different spiral vortices interrupted by "defects" are evident in Fig. 1(a). The IPS flow pattern rotates approximately as a solid body with a speed $\sim\Omega_a/3$, roughly equal to the v_ϕ at the r where the spirals have maximum amplitude. Defects migrate slowly through the flow, and their advective time-scale is comparable to the burst period. The average axial wavelength of a single vortex pair is ~ 0.9, consistent with nearly round vortices confined to $r < r^*$ and with experimental values. These properties of interpenetrating spiral flow are independent of initial conditions.

In all of our calculations, once the IPS flow is established, cycles of turbulent bursts begin. The onset of a turbulent burst is abrupt, bursting everywhere almost simultaneously. Large fluctuations occur on scales much smaller than the spiral vortices [Fig. 1(c)] and on time scales less than $T_{\mathrm{IC}}/10$, where T_{IC} is the inner cylinder rotation period. We quantify this as follows: the velocity is represented as a Fourier series $\mathbf{v} = \sum_{j,k} \tilde{\mathbf{v}}_{jk} \exp(ij\phi) \exp(ik2\pi z/H)$. We define a "large-scale" energy $E_L = \sum_{|j|<\hat{J},|k|<\hat{K}} \int_r |\mathbf{v}_{jk}|^2 r dr$ and a "small-scale" energy $E_S = \sum_{|j|\geq\hat{J},|k|\geq\hat{K}} \int_r |\mathbf{v}_{jk}|^2 dr$, with $\hat{J}$ and $\hat{K}$ chosen to correspond to the scale of a single vortex. The distribution of energy over small vs large scales is obtained by comparing E_S and E_L to their time-averaged values $\tilde{E}_S$ and $\tilde{E}_L$. At $R = 1.2R_c$ and during the laminar part of the cycle, $E_L \sim \tilde{E}_L$ and $E_S \sim 0.1\tilde{E}_S$. During the turbulent part, $E_L \simeq 0.1\tilde{E}_L$ and $E_S \simeq 10\tilde{E}_S$. Because the small scales of the burst are efficient at dissipating energy, the rate of viscous dissipation $\dot{E}_{\mathrm{diss}}(t)$ also serves as a good signature of a burst; it rises at onset, peaks when the turbulence is at a maximum, and drops when the turbulence collapses (Fig. 2). Once the burst begins to collapse, it quickly disappears throughout the entire flow. The flow re-establishes its laminar IPS spatial structure and the burst cycle repeats. At $R = 1.18R_c$, our calculations show that the period of the cycle is $T = 2.2T_{\mathrm{IC}}$ with $\sigma = 0.8T_{\mathrm{IC}}$ (based on computations of 15 burst cycles).

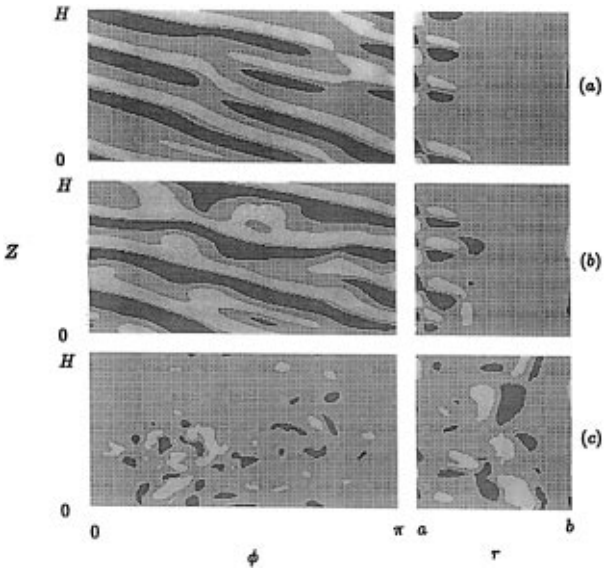

FIG. 1. Vorticity $\omega_\phi \equiv \hat{\mathbf{e}}_\phi \cdot (\nabla \times \mathbf{v})$ at three times with $R = 1.18R_c$ and $H = 3.68$. In the left column ω_ϕ is plotted in the (ϕ, z) plane at $r = a + 0.15$, and in the right column ω_ϕ is plotted in the (r, z) plane at $\phi = 0$. (a) Laminar spirals at $t = 1.25$. (b) The flow just before onset of a burst at $t = 16.25$. (c) The turbulent flow at $t = 45$. Each frame is scaled independently; black indicates $\omega_\phi > 0$, white $\omega_\phi < 0$, and all values of $|\omega_\phi|$ less than 20% of the maximum are grey. In a movie, the secondary mode is visible in (b), in the (ϕ, z) plane as a "lump" on each vortex that travels in the $-\phi$ direction.

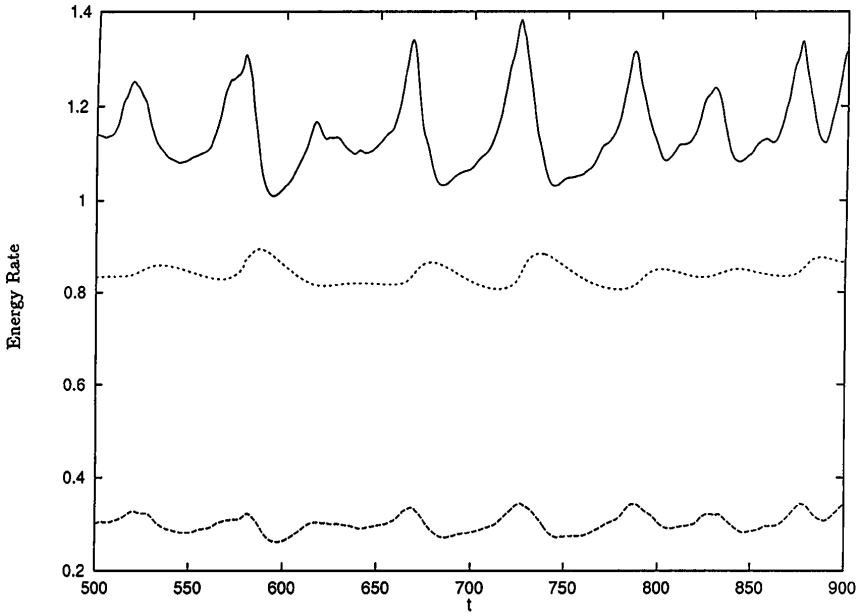

FIG. 2. $\dot{E}_{\rm diss}$ (solid), $\dot{E}_a$ (dashed), and $\dot{E}_b$ (dotted), all defined in the text, as functions of time during three burst cycles. $R = 1.16R_c$; $H = 3.68$. The increased values of $\dot{E}_{\rm diss}$ correspond to the turbulent bursts. $\dot{E}_b/\dot{E}_a \simeq 3$ because $|\mu\eta^{-3}| \simeq 3$.

Careful analysis of the flow just before the burst begins, supported by numerical experiment [5], has shown that the onset of turbulence is correlated with a secondary instability of the IPS. Based on symmetry, the spiral flow in Eq. (1) has linear Floquet eigenmodes of the form $e^{s't}e^{im'(\phi-c't)}e^{i2\pi z/\lambda'}\mathbf{g}$ where $\mathbf{g}$ has the symmetry of the spiral flow. We have confirmed this numerically and shown that at $R = 1.2R_c$, the spiral vortex flow with $H = 3.68$, $\lambda = H/4$, and $m = 4$ is supercritically unstable to a Floquet mode with $m' = 4$, $\lambda' = H$, and $c' = -0.366\Omega_a$. A new equilibrium that is quasiperiodic in time should branch from the bifurcation point and will be of the form [4]

$$\mathbf{v}_{\rm qp}(r,z,\phi,t) = \sum_{n=-\infty}^{\infty}\sum_{k=-\infty}^{\infty}\mathbf{a}_{n,k}(r)e^{in[2\pi z/\lambda+m(\phi-ct)]} \times e^{ik[2\pi z/\lambda'+m'(\phi-c't)]}. \quad (2)$$

This flow is *not* observed in laboratory experiments, nor in numerical experiments that are not artificially constrained. For example, if we impose four-fold, azimuthal symmetry then $\mathbf{v}_{\rm qp}$ as given by Eq. (2) becomes a stable equilibrium. When the symmetry constraint is removed, turbulent bursts begin, implying that the quasiperiodic equilibria are unstable. To pursue this, we prepared an initial condition at $R = 1.20R_c$ with $H = 3.68$ consisting of a spiral vortex (with $\lambda = 0.92$ and $m = 4$) added to a small amount of noise. The flow (with no imposed symmetry) grows into a spiral vortex flow $\mathbf{v}_{\rm sv}$ and develops a modulation due to an unstable Floquet mode. The flow is of the form given by Eq. (2), but the coefficients $a_{n,k}$ continue to grow in time. Note that if the modulation is of order ϵ, then to order ϵ^2 the unstable spiral vortex flow $\mathbf{v}_{\rm sv}$ is given by the $k = 0$ terms (the set $\mathbf{a}_{n,0}$) in Eq. (2), and the linear Floquet mode is given by the $k = 1$ terms (the $\mathbf{a}_{n,1}$). We found the $\mathbf{a}_{n,0}(r)$ are localized in the inner region, while the Floquet components, $\mathbf{a}_{n,1}(r)$, are localized at r slightly greater than r^*. The $a_{n,k}$ grow until $\mathbf{a}_{n,1}$ reaches a critical value at which point there is a turbulent burst. This burst is indistinguishable from the bursts that appear in the chaotic IPS flow. After the burst, the flow relaminarizes to IPS, and the cycle repeats with no memory that the initial condition was a nonchaotic flow. From this calculation we conclude that the chaos of the IPS flow is not necessary to create a turbulent burst. It also establishes the form of the secondary instability, which can then be compared with the instability of the more complex IPS.

We argue that when the quasiperiodic modulation $\mathbf{a}_{n,1}(r)$, which peaks near r^*, excedes a critical value, it "triggers" the finite-amplitude unstable shear flow in the outer region. In support of this argument, in our numerical calculations we have found that turbulent bursts are *always* immediately preceded by a modulation having the same characteristics as the Floquet mode in (2). Visually, the modulation appears as a wavy deformation of the spiral vortices that travels in the $-\phi$ direction, i.e., in the same direction as the flow in the outer region, and has its maximum amplitude just outside r^* [Fig. 1(b)]. This modulation has not been reported previously. It can be identified quantitatively by decomposing the flow into the form of Eq. (2). (This is complicated by the fact that the IPS is made of competing $\mathbf{v}_{\rm qp}$ with different values of m, m', λ, and λ'; however, for the largest amplitude spiral modes, the corresponding Floquet mode can generally be identified.) Using this decomposing at $R = 1.18R_c$, the phase speed c' of the modulation is $\sim -0.4\Omega_a$, roughly independent of m, m', λ, and λ', and once again corresponds to the value of v_ϕ at the radius

where the modulations have maximum amplitude. It produces a peak in the flow's power spectrum at frequency $\sim 2\pi/0.6T_{\rm IC}$ at $R = 1.18R_c$. After being identified in our calculations, this peak (and corresponding spatial modulation) has been tentatively confirmed in laboratory experiments [2] as appearing prior to each turbulent burst.

The collapse of the burst is explained by Fig. 2 which shows the dissipation rate $\dot{E}_{\rm diss}(t)$ and the energy input rates from the torques at the inner and outer cylinders, $\dot{E}_a$ and $\dot{E}_b$. Here, $\dot{E}_a \propto -\partial_r \overline{\Omega}$ and $\dot{E}_b \propto -(\mu\eta^{-3})\partial_r \overline{\Omega}$, where $\Omega \equiv v_\phi/r$, the derivatives are evaluated at the respective boundaries, and a bar over a quantity indicates an average over ϕ and z. The total rate of change of energy is $\dot{E}_a + \dot{E}_b - \dot{E}_{\rm diss}$. Figure 2 shows that during a burst $\dot{E}_a + \dot{E}_b < \dot{E}_{\rm diss}$, so the flow loses energy. Moreover, $\dot{E}_a + \dot{E}_b$ does not rise until after the burst collapses. To understand the burst's source of energy, define the velocity fluctuation $\mathbf{v}' \equiv \mathbf{v} - \overline{\mathbf{v}}$, its energy as $E' \equiv \frac{1}{2}\int |\mathbf{v}'|^2 dr^3$, the mean energy as $\overline{E} \equiv \frac{1}{2}\int |\overline{\mathbf{v}}|^2 dr^3$, and total energy as $E' + \overline{E}$. The torques at the walls do not directly feed the E'; the energy in E' comes from (or goes to) $\overline{E}$ via nonlinear interactions, so that any increase in E' corresponds to a decrease in $\overline{E}$. However, E' decreases directly (i.e., without changing $\overline{E}$) via viscous dissipation. During a burst E' increases, yet the small scales in $\mathbf{v}'$ rapidly dissipate E'; hence, there is a rapid transfer of energy from $\overline{E}$ to E'. This is possible because during the laminar part of the cycle $\overline{E}$ is large due to the differential rotation of $\overline{\mathbf{v}}(r)$. For a fixed value of angular momentum, the minimum energy flow is solid body rotation about the z axis. During a burst $\mathbf{v}'$ stirs the fluid which mixes and homogenizes the $L(r)$, making $\overline{v}_\phi$ rotate more like a solid body. This allows energy to be transferred from $\overline{E}$ to E' and is the burst's energy source. Only a finite amount of energy is stored in the flow's differential rotation, so after it is exhausted the burst collapses, the flow relaminarizes, and the cycle begins again.

To summarize, our conceptual model of turbulent bursts divides the flow into inner and outer regions. The outer region is centrifugally stable and physically similar to a plane-parallel shear flow. It contains most of the total flow's energy, and its local Reynolds number suggests that it is subcritically unstable. The inner region is centrifugally unstable to the formation of IPS, a chaotic flow consisting of spiral Taylor vortices with different helicities and wave numbers. The IPS flow is linearly unstable to quasiperiodic modulations (Floquet modes) which peak at radii just greater than r^*, the interface between the two regions. When the growing modulation exceeds a critical value, it acts as a finite-amplitude trigger for the outer flow. Once triggered, the entire flow bursts into turbulence. The burst collapses because its small scales dissipate energy quicker than it can be replenished. The flow relaminarizes, the instabilities are re-established, and the cycle repeats.

This model leads to quantitative predictions for the durations of the laminar part τ_L and the turbulent part τ_T of the cycle. τ_L is determined by the linear growth rate s' of the Floquet mode; hence $\tau_L \propto 1/s' \propto (R - R_c')^{-1}$, where R_c' is the critical value where the spiral vortex flow becomes unstable to quasiperiodic Floquet modes. (Note $R_c' \simeq R_c$.) τ_T depends on the available energy stored in the flow's differential rotation $\overline{v}_\phi(r)$ which is approximately independent of $R - R_c'$. Laboratory measurements [1] following the original submission of this Letter have verified these predictions as well as the existence of a growing Floquet mode just prior to each burst.

In our model, the flow in the inner region acts as a low-dimensional dynamical system that is coupled to and triggers a second dynamical system governing the outer shear flow which is high-dimensional and turbulent. This picture differs substantially from other models, such as that of Aubry *et al.* [9] for bursts in wall-bounded flows, based on a single low-dimensional system. In the latter, large amplitude fluctuations (bursts) may appear due to heteroclinic cycles, but use of the word "turbulence" is unrealistic as the low-dimensional system cannot produce any spatial disorder. Our conceptual model of bursts also applies to the intermittent cycles found in computations of spatially periodic channel flows [8,10] which, in turn, have been argued [8] to be good models of the spatially intermittent turbulent bursts seen generically in boundary layers. Thus, our conceptual model is likely to be representative of the general phenomenon of formation and breakdown of structures in shear flows.

We thank F. Hamill, H. L. Swinney, and S. Edwards. Our work was supported by NSF-CTS-8906343, by NSERC-WFA0138795, and by a Cray Grant Award at the San Diego Supercomputer Center.

[1] C. D. Andereck, S. S. Liu, and H. L. Swinney, J. Fluid Mech. **164**, 155 (1986); D. Coles, J. Fluid Mech. **21**, 385 (1965).
[2] C. F. Hamill, A. A. Predtechensky, E. Sha, and H. L. Swinney, 9th International Couette-Taylor Workshop, University of Colorado, Boulder, CO, August 7–10, 1995.
[3] P. S. Marcus, J. Fluid Mech. **146**, 45 (1984).
[4] K. T. Coughlin and P. S. Marcus, J. Fluid Mech. **234**, 19 (1992).
[5] K. Coughlin and P. S. Marcus (to be published).
[6] P. G. Drazin and W. H. Reid, *Hydrodynamic Stability* (Cambridge University Press, Cambridge, 1981).
[7] Finite axial boundaries create weak, large-scale Ekman cells which suppress the centrifugal instability and increase R_c and change the bifurcation sequence. See [5].
[8] J. Jimenez and P. Moin, J. Fluid Mech. **225**, 213 (1991).
[9] N. Aubry, P. Holmes, J. Lumley, and E. Stone, J. Fluid Mech. **192**, 115 (1988).
[10] K. Coughlin, J. Jimenez, and R. Moser, in *Proceedings of the 1994 Summer Program*, Center for Turbulence Research, Stanford University (1995), p. 229; K. Coughlin, J. Fluid Mech. (to be published).